Chapter 2
A Hadronic Collision

As explained in Chap. 1, the theory of QCD is able to explain a wide collection of phenomena in particle physics, initiated by strong interactions between partons and consisting in final states of hadronic jets. Many QCD predictions concerning deep inelastic scattering of electron beams colliding on protons and jet physics give a good agreement over a large number of measurements. It becomes thus crucial to study how partons interact between each other at high energies, namely to study collisions between partons. Since partons are not free in nature due to the confinement property, the most natural way to make partons collide is to use beams of particles, for instance protons, which contain quarks and gluons (see Chap. 1). In order to give a satisfactory view of a pp collision, or more generally of a hadronic collision, the simple picture of only two interacting partons is not sufficient. This is due to the fact that the colliding hadrons are composite objects: the two partons, one for each colliding hadron, that take part in the interaction, are accompanied by other quarks and gluons that rearrange themselves after the collision in colourless objects under the effect of QCD. In addition, the possibility that additional partons of the two colliding hadrons may interact, is not excluded. The complexity of a hadronic collision can be represented, for simplicity, by distinguishing two different elements:

- the Hard Scattering which represents the hardest part of the collision, where two partons in the initial state interact by exchanging a high transverse momentum (see Sect. 2.2);
- the Underlying Event (UE) which describes the whole remaining part of a hadronic collision, namely the interaction and the evolution of the partons that do not take part in the hard scattering (see Sect. 2.4).

In this chapter, these two components are discussed. Particular attention is given to how they are combined in the whole picture of a hadronic collision, and how they are implemented in simulations. The focus is then drawn to the main topic of this thesis, namely the Multiple Parton Interactions: phenomenology and experimental results are described from the literature and an introduction to the physics interest of the experimental measurement, described in the following chapters, is provided.

© Springer International Publishing Switzerland 2016

P. Gunnellini, *Study of Double Parton Scattering Using Four-Jet Scenarios*,
Springer Theses, DOI 10.1007/978-3-319-22213-4_2

2.1 Formalism of a Hadronic Cross Section: The Factorization Theorem

One of the most important quantities to evaluate in a hadronic collision is indeed the cross section σ of a certain process: it represents the probability that the two hadrons interact and give rise to that specific process. For any cross section calculation, the fact that the hadrons are composite is treated by the theory with an idea, which combines the two components of the collision (hard scattering and UE). It is assumed that the hard scattering process occurs in a timescale much shorter than the one characterizing the interactions of the other "spectator" partons. In a pictorial view, the hard probe takes a snapshot of the projectile hadron structure at the instant of the interaction, with the other partons, which do not participate, seen as "frozen". This is the basic idea of the factorization theorem [1], that states the independence between short-distance hard processes, included in the hard scattering, and softer components, contained in the UE. Mathematically, this translates into the factorization of the hard scattering and the UE parts. Thus, it is possible to write any hadron-hadron cross section as a product of two non-perturbative process-independent parton density functions (PDF), one for each of the colliding protons, and a perturbative parton-parton cross section.[1] In a compact formula, this can be expressed as:

$$d\sigma_{\mathrm{h_1 h_2}} = \sum_{\mathrm{i,j}} \int_0^1 dx_1 \int_0^1 dx_2 \sum_{\mathrm{f}} \int d\Phi_{\mathrm{f}}\, f_{\mathrm{i/h_1}}(x_{\mathrm{i}}, \mu_{\mathrm{F}}^2)\, f_{\mathrm{j/h_2}}(x_{\mathrm{j}}, \mu_{\mathrm{F}}^2) \frac{d\sigma_{\mathrm{ij\to f}}}{dx_{\mathrm{i}} dx_{\mathrm{f}} d\Phi_{\mathrm{f}}} \tag{2.1}$$

where $x_{\mathrm{i,j}}$ is the fraction of longitudinal momentum of the colliding hadrons carried by the parton $(i, j), i, j$ are indices that run over all possible parton types in the incoming hadrons, while f stands for all possible partonic final states with Lorentz-invariant phase space Φ_{f}. The parton density function, $f_{\mathrm{i/h_1}}$, parametrizes the distributions of the partons inside each hadron: it represents specifically the probability of finding a parton of flavour i at a certain longitudinal momentum fraction x_{i}, when the hadron, that contains it, is probed at a certain scale μ_F. The PDF are non-perturbative functions which are not calculable a priori. However, they can be extracted from fits to the data, mainly from ep collisions, and various PDF sets are available for each parton flavour going down to very low scales. Then, from each initial scale, it is possible to evaluate the PDF evolution to any other scale through the evolution equations defined in Chap. 1. Examples of these sets are CTEQ6L1 [2], MRST [3] and HERAPDF [4]. Figure 2.1 shows some examples of currently used PDF sets; the variation of the gluonic distribution function is also shown at different scales. It is shown that the valence quarks, namely the quarks that determine the macroscopic properties of a hadron, are mostly present inside the proton at high x values (>0.01), while the gluons are almost absent. In the low-x region, instead, the gluon densities increase rapidly and

[1] In a lepton-hadron collision, this formalism is still valid but only one parton density function is obviously included.

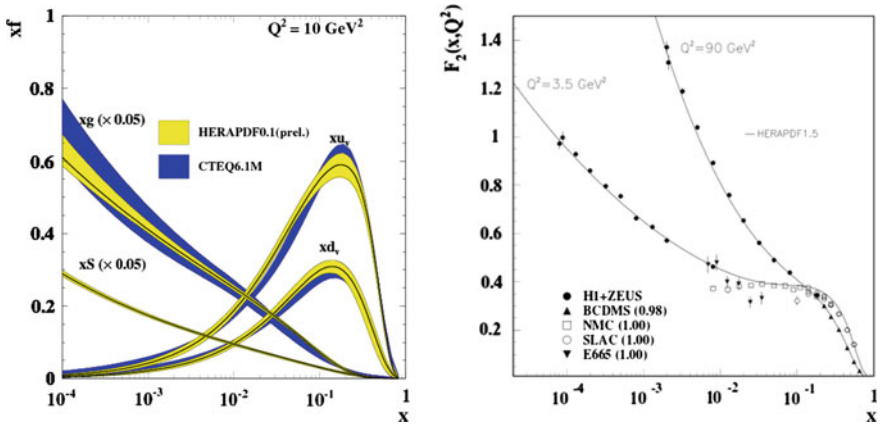


Fig. 2.1 (*Left*) Parton distribution functions obtained by the HERAPDF and CTEQ collaborations at a scale $Q^2 = 10\ GeV^2$ with uncertainty representing the 68 % confidence level [5]. (*Right*) Gluon parton distribution functions measured at two different scales, $Q^2 = 3.5\ GeV^2$ and $Q^2 = 90\ GeV^2$, by the HERAPDF collaboration with deep inelastic scattering data [6]

they dominate over the quarks by several orders of magnitude. Antiquark and heavy quark PDF are very small compared to gluons and light quarks at all scales.

In the partonic cross section only the hard scattering part is considered, where one parton of a colliding hadron interacts with another parton of the other hadron and it is calculable within the perturbation theory as a series in the running coupling α_S. A more detailed description is provided in Sect. 2.3. The separation line between these two components, namely the partonic cross section and the PDF, is the so-called "factorization scale" (μ_f). The value of the factorization scale is arbitrary but a common choice is to take μ_f equal to the hard scattering scale [7]. However, no universal value can be identified and it is always important to evaluate the effects of changes in μ_f for the calculated cross section values.

A further assumption that is generally done inside the formalism of the factorization theorem is that the transverse momenta of the incoming partons, involved in the hard interaction, are neglected; this is called "collinear approximation" and it is motivated by the fact that at high energy scales, transverse momenta of the partons in the initial state can be neglected. This kind of approach is able to describe a wide range of data. However, it starts to fail when gluons at low-x values are probed: in fact, low-x values translate into longitudinal momenta which are no longer larger than the transverse momenta of these partons. In this region, a dependence on the partonic transverse momentum needs to be explicitly expressed in both the partonic cross section and in the PDF. In particular, in this case, uPDF need to be used for calculations in the low-x regime.

2.2 Hard Scattering and Matrix Element

In the cross section formulation, the matrix element (ME) is the mathematical expression which represents the hard scattering occurring during the collision. The hard scattering might be thought of as an interaction between two partons in the initial state, which produces a final state with two or more partons. Considering an arbitrary final state F and a state f with only two final partons, the generic total cross section, defined in Eq. 2.1, might be expanded, by including explicitly all orders, as:

$$\sigma_{\mathrm{F}} = \sum_{\mathrm{k}=0}^{+\infty} \int d\Phi_{\mathrm{f+k}} | \sum_{\mathrm{l}=0}^{\infty} M_{\mathrm{f+k}}^{(\mathrm{l})} |^2 \tag{2.2}$$

Note that the terms relative to the proton PDF have been dropped for compactness and the focus is drawn to the hard scattering part. $\Phi_{\mathrm{f+k}}$ is the phase space for a final state f with k additional partons (legs), while $M_{\mathrm{f+k}}^{(\mathrm{l})}$ is the ME, namely the amplitude, for producing the same final state f with k legs and with l additional loops. A leg is a real correction to the total cross section, while a loop is called a virtual correction, because it does not produce any particle in the final state but only enters in the calculations (see Fig. 2.2). By choosing certain values for legs and loops, namely for k and l respectively, different processes are included in the analytical calculation of the cross section: in particular, it is generally said that the calculation is performed at a fixed order in α_{S}. The order in α_{S} refers to the number of QCD vertices included in the calculation of $M_{\mathrm{f+k}}^{(\mathrm{l})}$. Real and virtual corrections increase the order in α_{S} of, respectively, one and two units. Increasing the number k means that a higher number of real partons is included in the final state, while with the number l, loop virtual corrections are taken into account into the cross section calculation, without increasing the number of partons in the final state. Depending on different choices on k and l, various cases can be identified for the final state f:

- $k = 0, l = 0$: production of the final state f at Leading Order (LO);
- $k = n, l = 0$: production of $f + n$ jets at Leading Order (LO);
- $k+l \leq n$: production of f at $\mathrm{N^nLO}$ which includes $\mathrm{N^{n-1}LO}$ for $f+1$ jet, $\mathrm{N^{n-2}LO}$ for $f + 2$ jets and so on until LO for $f + n$ jets.

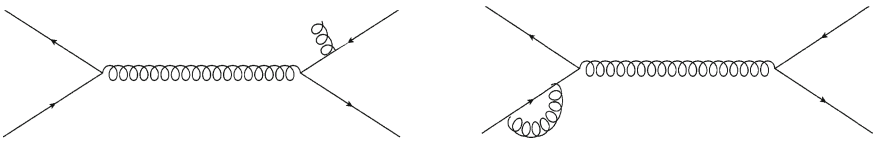


Fig. 2.2 Example of QCD diagrams of two initial quarks which annihilate into a gluon which further splits into two final quarks [8]: in the *left* plot, a real gluon is emitted by one of the final quarks, while in the *right* plot an initial quark emits and reabsorbs a virtual gluon. The *left* figure is an example of real correction to a $2 \rightarrow 2$ process, while the figure on the right includes a virtual correction for the same process

It is, for instance, referred to as LO $2 \to 2$ processes if $k = 0$ and $l = 0$, LO $2 \to 3$ processes if $k = 1$ and $l = 0$, and NLO $2 \to 2$ processes if k+l ≤ 1.

Since the cross section is an infinite sum in α_S, by choosing finite values for k and l, higher order contributions are left out from the matrix element calculation; however, they are not ignored but the *leading log* contributions are absorbed into the parametrization of the PDF and its evolution starting from a certain scale, given by μ_f. QCD calculations at LO normally suffer from large higher order corrections and scale uncertainties and the more terms are included into the matrix element calculation, the smaller the dependence on the choice of the factorization and renormalization[2] scales is. On the other hand, the degree of complication in the calculations increases dramatically with any further order that is added. A naive way to improve LO calculations is to correct them with an overall factor corresponding to the ratio of cross sections at NLO and LO for a given final state. This is the so-called "K-factor", defined as:

$$K = \frac{\sigma_F^{NLO}}{\sigma_F^{LO}} \tag{2.3}$$

By multiplying it to the LO cross section, virtual corrections are aimed to be corrected for and K-factors for several processes have been calculated [9]. A problem of this procedure is that often NLO calculations result in a shape change of the studied observable and this effect is not taken into account by the K-factor.

2.2.1 Matching Between Matrix Element and Parton Shower

Since an analytical calculation of the ME at all orders in α_S is not doable, the missing diagrams which are not included, are computed by the PS. The issue of combining ME calculations with the PS is addressed by the "matching procedure". An important role of a matching procedure is to remove the possibility of double counting terms present in both the matrix element and the PS expansion. There are many methods to perform that. After the production of a $2 \to 2+n$ process in the ME, the PS is invoked for each of the final legs. The most used matching schemes [10] are the CKKW [11] and the MLM [12]: the former is based on a shower veto, the so-called "truncated shower", which generates additional partons only below the lowest scale of the ME, while the latter works with an event rejection, where an event is discarded if a parton is emitted above the scale of the partons in the ME. Additional ways have been also recently developed, mainly to perform the matching of NLO ME with PS: these are the POWHEG method [13], based on the generation of the first hard emission which sets the upper scale for the rest of the shower, and the MC@NLO method [14], where some part of the shower is subtracted from the total cross section to avoid

[2]The renormalization scale is an arbitrary parameter introduced in the theory to treat divergences appearing in loop diagrams.

double counting. These methods are widely used in Monte Carlo event generators (see Sect. 2.5), to get predictions for higher-order ME or NLO ME, interfaced with PS and UE.

2.3 Definition of the Underlying Event and Multiple Parton Interactions

The UE is a very important component in a hadronic collision, including most of the occurring partonic interactions; it can be easily represented as everything that happens in the collision, but the hard scattering. This general definition stems from the fact that it includes all the different elements which underlie (as the name suggests) the primary hard interaction. In particular, different subphenomena are grouped under the name of the UE:

- Initial- and final-state radiation which includes the emission of additional particles by partons in the initial or in the final state, namely before or after the hard scattering;
- Beam-beam remnants (BBR) which group the colour interactions undergone by the spectator partons in each of the two colliding hadrons;
- Multiple parton interactions (MPI) which contain the whole of additional interactions between partons of the colliding hadrons, occurring together with the hard scattering.

The contribution provided by these components to the collision events is generally softer than the hard scattering, but still calculable within the perturbative framework. A sketch of a hadronic collision as a whole is shown in Fig. 2.3 where the different components are represented in various colours.

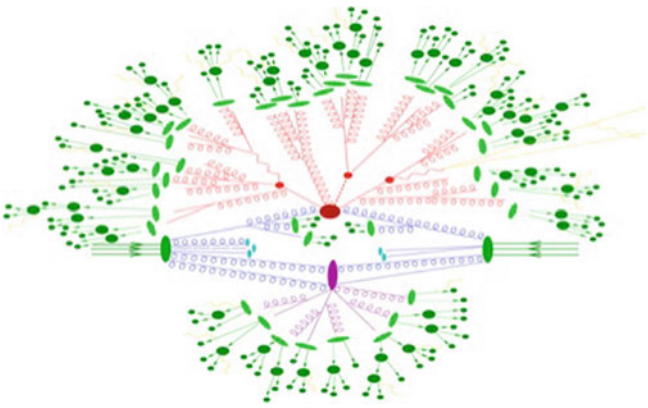


Fig. 2.3 Sketch of a hadronic collision with all the contributions included [15]: the hard scattering is represented in *dark red*, the initial- and the final-state radiation is pictured respectively in *blue* and *light red*, a MPI event in *violet* and the beam remnants are sketched in *cyan*. At the very end of the *lines*, the hadronization products are shown in *light* and *dark green*

The initial- and final-state radiation comprises quarks and gluons that are emitted by the partons that take part in the hard scattering respectively before and after the interaction. As seen in Sect. 2.2, if initial- and final-state radiation is included in the ME calculation by adding additional legs, they have to be considered as a part of the hard scattering; this case mainly addresses n-objects final states, with $n > 2$, at large p_{T}. However, in general, for $2 \rightarrow 2$ processes, initial- and final-state radiation needs to be considered under the UE classification, and plays a key role in both soft and hard UE components. The effect and the impact of initial- and final-state radiation has been studied at leptonic and hadronic colliders. It is possible to disentangle the corresponding contributions: for the study of final-state radiation, it is important to select a leptonic initial state with a "coloured" final state (like in [16], for quark production in electron-positron collisions). A hadronic initial state with a leptonic final state (like in [17], for Drell-Yan production in pp collisions) is necessary for measurements related to initial-state radiation.

The BBR are the outcome of the rearrangement of the "spectator partons" of the two colliding protons. The spectator partons are the ones that do not participate in the hard scattering. Since they carry colour charge, they need to form coloured objects after the hard scattering. The main contribution of the BBR is concentrated very closely towards the initial directions of the incoming protons and it takes most of the energy of the collision energy. Hence, it is often detected only in the part of the detectors close to the beam pipe. Beam-beam remnants mainly contribute to the soft part of the UE.

The MPI describe the possibility to have more than one distinct and simultaneous parton interaction inside the same hadronic collision. The MPI are mainly due to the compositeness of the incident hadrons that may be thought of as bunches of partons whose wave functions overlap with each other. In presence of a hard partonic collision between the two hadrons, there is a high probability that the spectator partons experience a hard interaction as well; the scale of a MPI is, indeed, lower than the scale of the hard scattering but large enough to have a relevant and considerable contribution to the final state. MPI predominantly contribute to the soft and semi-hard UE components but some of these additional interactions, in a lesser extent, can reach a high scale which gives also a hard component to the UE (see Sect. 2.5).

Historically, the existence of the MPI has been conjectured from the observation that the total parton-parton cross section, σ_{hard}, tends to rapidly increase at low values of exchanged transverse momentum. In fact, if σ_{hard} is represented as an integral of a generic partonic cross section, $\hat{\sigma}$, over the exchanged transverse momentum between the two partons, from an initial cut-off to the maximum value allowed by energy-momentum conservation, it can be written as:

$$\sigma_{\mathrm{hard}}(p_{\mathrm{T}_{\mathrm{min}}}) \propto \int_{p^2_{\mathrm{T}_{\mathrm{min}}}}^{s/4} \frac{d\hat{\sigma}}{dp^2_{\mathrm{T}}} dp^2_{\mathrm{T}} \propto \frac{1}{p^2_{\mathrm{T}_{\mathrm{min}}}} \tag{2.4}$$

where $p_{\mathrm{T}_{\mathrm{min}}}$ is the threshold of the exchanged transverse momentum between the two partons. It is obtained that, at $p_{\mathrm{T}_{\mathrm{min}}}$ values around 3–5 GeV which is still in the

perturbative regime, σ_{hard} exceeds the non-diffractive cross section σ_{nd}, measured to be about 70 mb at 7 TeV [18, 19]. Formulated in this way, this might seem indeed a paradox; it would result that the total pp cross section, at a relatively high scale, is lower than the cross section of two of their constituents. The possibility of having MPI solves this issue. If more than one partonic interaction in a hadron-hadron collision is assumed, the consistency is actually restored. In fact, σ_{nd} indicates the hadron-hadron cross section, conceived as a whole of multiple interactions where partons from the different colliding hadrons might simultaneously interact between each other. In this new formulation, σ_{hard} is not an event but a jet quantity, since partons are not free but only contained in hadrons; σ_{hard} becomes meaningful to give an estimation of the number of MPI through the relation:

$$\langle n \rangle = \frac{\sigma_{\text{hard}}(p_{\text{T}})}{\sigma_{\text{nd}}} \tag{2.5}$$

where n follows a Poisson distribution. However, σ_{hard} still diverges for $p_{\text{T}} \to 0$. This would mean that the number of MPI becomes rapidly infinite when going to very low exchanged p_{T}. This problem is solved by introducing effectively a p_{T} cut-off in the formula for σ_{hard}, motivated by the fact that, since the hadrons are colour-neutral objects and the parton wavelength increases at lower p_{T}, the partons at relatively low p_{T} ($\sim$1 GeV) can no longer resolve the individual colour charges and the coupling is decreased in this region. This matter is equivalent to include a limit in the gluon density function, in order to tame its increase at low-x values: this mechanism goes under the name of "gluon saturation" [20].

The effects of MPI naturally tend to increase for higher energies, where the low-x region becomes accessible and where the parton densities are very high. This is why they have been measured at past and present colliders and they gain more and more importance and attention at future ones [21].

2.3.1 Measurements of UE and MPI at Colliders

The concept of MPI has been successfully applied to describe the properties of soft collisions, as well as the details of jet final states. A wide collection of measurements that exhibited sensitivity to MPI is available at several hadron colliders and at various energies. In particular, the presence of MPI tends to increase the general event activity, in terms of number of particles and energy. One of the most popular ways to measure and to estimate the MPI contribution is the measurement of the UE "a-la-Rick-Field" [22]. This method has been introduced for the first time in the CDF collaboration and then applied to similar measurements at other colliders. It consists of measuring the event content in terms of charged particles in different regions of the phase space relative to the direction of the hardest objects in the event. In particular, the hard object (a jet in case of measurements of UE in hadronic events, a dimuon pair in case of Drell-Yan events) identifies a direction ϕ_{hard} in the transverse plane. The

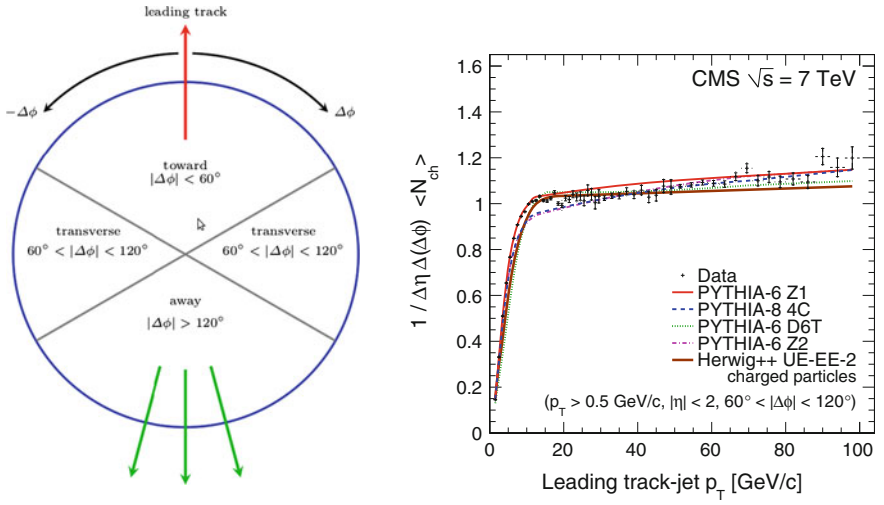


Fig. 2.4 (*Left*) Transverse plane division used for measurements of UE contribution [26]: the direction and the scale of the hard scattering are defined by the leading object in the event and the xy-plane is thus divided in three regions, depending on their azimuthal angle with respect to that object. These regions are called toward, transverse and away. (*Right*) Example of UE measurement performed with the method "a-la-Rick-Field" [25]: charged particle multiplicity, as a function of the p_T of the leading track, measured at the CMS experiment at 7 TeV, in the transverse region. The measured curve is characterized by a rising part at low scales and a plateaux region for increasing ones

transverse plane is then divided into four regions, as shown in Fig. 2.4 (left), which are commonly referred to as:

- toward region: $|\phi - \phi_{\text{hard}}| < \pi/3$
- transverse region: $\pi/3 < |\phi - \phi_{\text{hard}}| < 2\pi/3$
- away region: $|\phi - \phi_{\text{hard}}| > 2\pi/3$

where ϕ is the azimuthal angle considered in the transverse plane. In these regions, the observables which are generally measured are the multiplicity and the p_T sum of the charged particles in every event.[3] Measurements of these observables are performed as a function of the p_T of the hard object: this gives a dependence on the scale of the scattering that may be easily thought of as the centrality of the collision between the two hadrons. Assuming that the direction of the hardest objects may be identified in good approximation with the direction of the hard scattering, every region in the transverse plane is affected by different components of the collision. The toward region contains the products of the hard scattering and most probably the contribution of the initial- and final-state hard radiation. The transverse region contains the products of the MPI and the BBR along with additional soft radiation.

[3]These observables are chosen because they are experimentally accessible down to low p_T and easy to measure with a tracking system.

The away region measures the area of the recoiling object, namely the opposite region with respect to the leading object. A more sophisticated approach has been also recently considered for this type of measurements by considering separately the two transverse regions in terms of event content [23].[4] This approach, explained more extensively in Appendix D, helps to further separate the components that contribute to the content of the transverse region.

Hadronic event measurements have been performed as a function of the leading jet p_{T} and of the leading track p_{T} by the CDF [24], the CMS [25] and the ATLAS [26] collaborations for different energies. The curves show always a rapid rise at low p_{T} and a plateaux region at higher p_{T} starting from 5–10 GeV, depending on the collision energy. All these measurements have shown the importance of the implementation of the MPI in the event generators to give a good and consistent description of the data. Predictions obtained without MPI significantly fail to reproduce the measurements. An example of this curve, which represents the charged particle multiplicity as a function of the hard scale, measured by CMS at 7 TeV, is shown in Fig. 2.4 (right).

Similar measurements have been performed for different processes occurring at the hard scattering, for instance with Drell-Yan events [17] and top-antitop quark pair production [27][5]; a very good description of the data is only achieved with models which include MPI. Other evidences of MPI come also from a wide collection of different measurements, related to jets [29], particle event contents [30] and energy flow [31]. Thanks to all these observations and measurements, the concept of MPI is well established and well received in the scientific community.

2.4 Double Parton Scattering

In a framework where the MPI are so important in order to explain such a big variety of measurements, even additional scattering at a larger scale may accompany the first hard interaction. In fact, nothing prevents a MPI to reach a scale comparable to the one of the hard scattering. If this occurs, with one additional hard scattering, the literature generally refers to a Double Parton Scattering (DPS).[6] The understanding of DPS is particularly relevant for the estimation of backgrounds in measurements of specific or rare physics channels, especially the ones involving jets in the final state. A good comprehension of the DPS dynamics is also of great help for the general phenomenology, with increasing importance for higher collision energies, and for the development of partonic models of hadrons. Likewise a MPI measurement which can be performed by looking at average observables, like charged particle multiplicity

[4] By separating them in the region with higher and lower activity, it is possible to disentangle even further the UE components.

[5] Also a UE measurement in $b\bar{b}$ pair events is planned in the CMS collaboration and studies at the generator level have been performed [28].

[6] Events with a higher number of additional interactions might be also considered and they are thus called "Triple, Quartic, .. Parton Scattering" but their contribution becomes very small. In this work, only the actual DPS will be treated.

or p_{T} event content, a detection of a DPS event is not possible in an event-by-event basis; however, it is possible to identify specific channels and region of the phase space where its contribution is enhanced. The possibility to produce high-p_{T} physics objects from DPS came up together with the concept of MPI and several phenomenological studies have been performed by scanning different channels and defining sensitive observables for its discrimination. Already in 1982 [32], a first attempt of DPS formalism for a multiquark scattering treatment was discussed and first ideas related to double Drell-Yan production [33] have been developed. Studies of sensitivity to DPS for various physics channels are widely documented in the literature: in pp collisions, four-jet final states [34–36], W-boson production associated with jets [37], di-boson [38] and double J/ψ [39] final states have shown promising outcomes for specific regions of the phase space. The capability to disentangle a DPS signal from the background is discussed in proton-lead [40, 41] and $p\bar{p}$ [42] collisions as well.

2.4.1 Theory of Double Parton Scattering

Double Parton Scattering phenomenology is based on the general expression for the cross section, introduced in Eq. 2.1, adapted for multiple scattering at the matrix element level. The new parton distributions include information of multiple parton structure of the proton and refer to the probability distributions of finding two partons with given longitudinal momentum fraction at a given scale and with a certain separation distance in the transverse plane; hence, these new PDF are called double parton distribution functions. In this formalism, $\sigma^{\mathrm{DPS}}_{(\mathrm{A,B})}$ is defined as the cross section of a DPS event in hadronic collisions, where two independent processes A and B occur simultaneously. It can be expressed as:

$$\sigma^{\mathrm{DPS}}_{\mathrm{A,B}} = \frac{m}{2}\Sigma_{\mathrm{i,j,k,l}} \int dx_1 dx_2 dx_1' dx_2' d^2b \Gamma_{\mathrm{i,j}}(x_1, x_2, b; t_1, t_2) \\ \Gamma_{\mathrm{k,l}}(x_1', x_2', b; t_1, t_2)\hat{\sigma}^{A}_{\mathrm{i,j}}(x_1, x_1', t_1)\hat{\sigma}^{B}_{\mathrm{j,k}}(x_2, x_2', t_2) \tag{2.6}$$

where $x_{1,2}$ ($x'_{1,2}$) are the longitudinal momentum fractions of the two partons of the first (second) proton, $t_{1,2}$ are the scales characteristic of the subprocesses A and B, and b is the distance parameter between the two partons. The two $\Gamma(x_1, x_2, b; t_1, t_2)$ represent the double parton distribution functions and the two $\hat{\sigma}$ are the inclusive partonic cross sections of the two processes. The quantity m is a symmetry factor that is equal to 1 if A = B, and 2 otherwise. This definition for $\sigma^{\mathrm{DPS}}_{\mathrm{A,B}}$ is process- and energy-independent. If the dependence on the transverse distance factorizes with the rest of the parton distribution, like:

$$\Gamma_{\mathrm{k,l}}(x_1', x_2', b; t_1, t_2) = D_{i,j}(x_1, x_2, t_1, t_2) \cdot F(b), \tag{2.7}$$

the equation becomes:

$$\sigma_{\mathrm{A,B}}^{\mathrm{DPS}} = \frac{m}{2\sigma_{\mathrm{eff}}} \Sigma_{\mathrm{i,j,k,l}} \int dx_1 dx_2 dx_1' dx_2' D_{\mathrm{i,j}}(x_1, x_2; t_1, t_2) \\ D_{\mathrm{k,l}}(x_1', x_2'; t_1, t_2) \hat{\sigma}_{\mathrm{i,j}}^{A}(x_1, x_1', t_1) \hat{\sigma}_{\mathrm{j,k}}^{B}(x_2, x_2', t_2) \tag{2.8}$$

with $\sigma_{\mathrm{eff}} = \left[\int d^2b (F(b))^2\right]^{-1}$. Note that $F(b)$ represents the dependence of the DPS cross section on the relative parton position inside the proton and it is thus referred to as "matter distribution". To further simplify the formalism, the double parton distribution functions can be reduced to two independent single ones, namely $D_{\mathrm{i,j}} = D_{\mathrm{i}} \cdot D_{\mathrm{j}}$, under the assumption of complete uncorrelation between partons of the same protons, and the DPS cross section can be finally expressed in the simple form:

$$\sigma_{(\mathrm{A,B})}^{\mathrm{DPS}} = \frac{m}{2} \frac{\sigma_{\mathrm{A}} \sigma_{\mathrm{B}}}{\sigma_{\mathrm{eff}}} \tag{2.9}$$

With these approximations, σ_{eff} carries information about the size of the partonic core of the proton and might be thought of as related to the transverse size of the proton. Its dimensions are the ones of an area (i.e. a cross section). In the most trivial approximation with no correlations between partons and assuming a uniform matter distribution, σ_{eff} should be equal to the total inelastic cross section ($\sim$70 mb).

It has been demonstrated in [43], that this formula remains valid only if inclusive scenarios are considered, namely selections where no vetoes are applied for additional objects in the final state and where a number of hard scatterings greater than two is allowed. If this is the case, then the resulting σ^{DPS} presents an explicit dependence on the impact parameter b and the formula needs to be modified [43].

However, under discussion is the possibility to improve the DPS picture and to leave out some of the currently adopted approximations. Indeed, it is questionable that hard scatterings in the same event may occur independently and without any correlation. Interesting conjectures have been published about the transverse impact parameter dependence in the double parton distribution functions [44–46] and spin correlations between the partons inside the same hadron [47–50]. Even though these theories are still at a speculative stage, they predict significant consequences in both the DPS cross section values and the event topology[7] and they could give many insights on the understanding of the hadron structure. The final goal is to find a consistent picture that would be able to explain multiple interactions at all possible scales, from soft ones to the ones with hard scatterings.

[7]For instance, in particular scenarios with large spin correlations between the initial-state partons, a modulation on the relative azimuthal angle of the final-state partons appears, while the inclusion of colour correlation adds extra colour factors to the DPS cross section which would change its absolute contribution.

2.4.2 Measurements of Double Parton Scattering at Colliders

Evidence for DPS events has been observed in various channels and at different energies. Final states involving four jets have been measured by the AFS collaboration at the CERN ISR [51], as well as $\gamma + 3$ jets by the D0 [52] and CDF [53] collaborations in $p\bar{p}$ collisions. More recently, the ATLAS [54] and CMS [55] collaborations have contributed with the W+dijet channel and the D0 collaboration with the γ+b/c jet+2 jets [56]. Furthermore, the double J/ψ production measurement performed by the CMS [57] and the LHCb [39] experiments may also be used to improve the understanding of DPS. Conclusions of this collection of measurements have been that the addition of a DPS signal in the simulation helps to get a better agreement with the data. All of them, except the double J/ψ measurement in CMS, have provided an estimate of σ_{eff} in the theoretical framework of Eq. 2.9, along with distributions that are sensitive to the DPS signal. The DPS-sensitive observables use information of the topology of the event and the configuration of the physics objects in the final state (see Chap. 4). A technique used for the extraction of the σ_{eff} in CMS and ATLAS, is the so-called "template method" and it is based on a fitting procedure to DPS-sensitive observables. Two templates are considered in the fit: one for the background and one for the DPS signal. From the relative fraction of the two templates that fit the observed results best, a determination of σ_{eff} can be performed. The application of this method will be treated in Chap. 11.

From the experimental point of view, it becomes important to provide measurements of observables sensitive to DPS and, from these data, to extract a value of σ_{eff} by following the definition provided in Eq. 2.9. Even if the approximations used in that case are too simplicistic, an extraction of σ_{eff} with these assumptions for different channels and different energies is meaningful: if results of σ_{eff} are different for the various channels, it would be a clear indication that this simplified model needs to be improved, e.g. by introducing correlations between the partons. The current situation of the measured σ_{eff} values for different channels and as a function of the collision energy, $\sqrt{s}$, is represented in Fig. 2.5. Uncertainties, mainly of systematic nature related to the extraction method, are rather big and they do not yet allow a conclusive statement about the channel and energy dependence. The value of σ_{eff} seems to be around 15–20 mb at $\sqrt{s} = 7$ TeV.

The work, described in this thesis, contributes in this research topic, by measuring DPS-sensitive observables for two channels involving jets in the final state: one with four jets, and one with two b-jets and two additional ones. A new approach for σ_{eff} extraction is described and applied for the first time to the measured channels. In the following Section, details of these two channels are described, with a particular focus on the physics interest related to DPS.

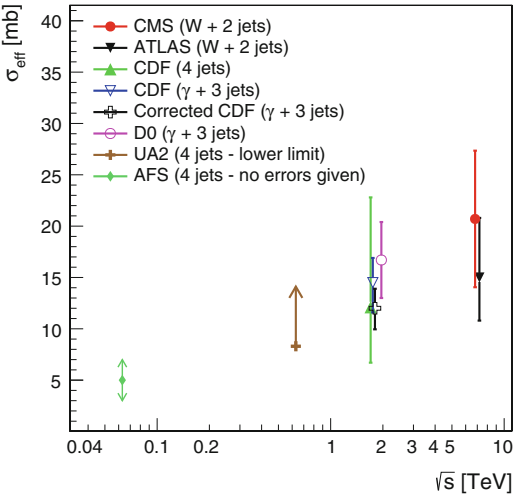


Fig. 2.5 Measured σ_{eff} values as a function of the collision energy [55]: data points come from measurements at different experiments. The physics channel used for the measurement is also indicated in the plot for each point

2.4.3 DPS in Four-Jet Channels

The physics channels which are described in this thesis are related to a four-jet scenario. Four jets might be produced by two different processes occurring in the collision: a Single Parton Scattering (SPS), represented in Fig. 2.6 with a pictorial view and with the specific Feynman diagrams, and a DPS, shown in the same way in Fig. 2.7. In SPS events, the four jets are produced by a single chain, with all jets coming from the hard scattering; in DPS, instead, two different chains emit the two pairs of jets in the final state. These two production mechanisms translate into

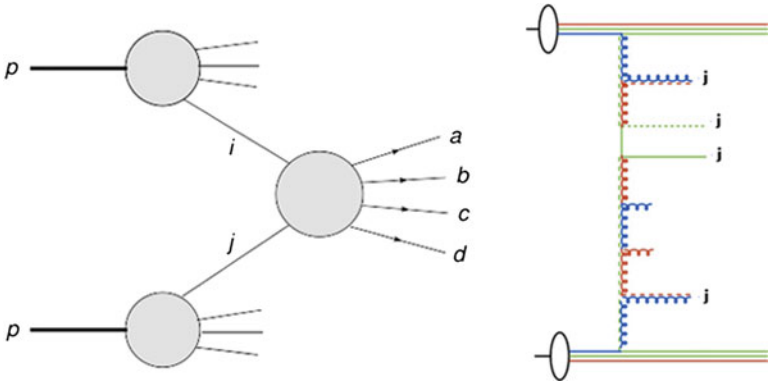


Fig. 2.6 A Single Parton Scattering event in a pp collision, with four jets in the final state. In the *left* plot, a sketch of the active partons (i, j) producing the four objects, (a, b, c, d), in a single chain, is represented, while in the *right* plot, the Feynman diagram of the process is shown

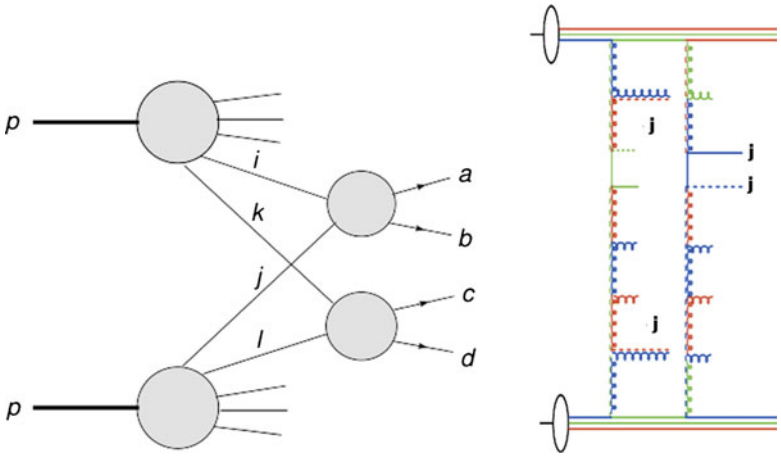


Fig. 2.7 A Double Parton Scattering event in a pp collision, with four jets in the final state. In the *left* plot, a sketch of the active partons (i, j) and (k, l) producing the four objects, (a, b) and (c, d), in two different chains, is represented, while in the *right* plot, the Feynman diagram of the process is shown

different configurations and topologies in the final state, with a higher correlation among the jets for SPS. Thus, by associating the jets into two pairs and investigating particular observables which are sensitive to the relative position of the jets, it is possible to separate the two different contributions. Quantitative studies about how to separate a DPS signal from a SPS background are presented in Chap. 4. In particular, two scenarios with four jets in the final state have been studied: one with exclusively four jets and one with two b- and two other jets. The possibility of tagging heavy-flavoured jets is very important for separating SPS and DPS, because it helps the association in pairs of the jets in the final state.

2.5 Monte Carlo Event Generators

The goal of a Monte Carlo (MC) event generator is to simulate everything that happens in a hadron-hadron collision. This includes the production of a hard scattering, the implementation of the PS related to the evolution of the partons and the UE. MC generators differ mainly in the implemented ME for the hard scattering process and in the UE simulation, namely how PS and MPI are produced. While in LO generators only $2 \rightarrow 2$ processes are calculated and the additional emitted partons are implemented through the PS, there are several cases where higher-order ME are implemented at the Born level. By including additional emissions in the ME, the exact kinematics and all the interference and helicity parton structures are taken into account. On the other hand, to calculate higher-order diagrams and loop corrections

is a very time consuming process and a compromise needs to be done. The corrections which are not included at the matrix element level are estimated through the PS. The PS is simulated in the current generators by defining a parton probability of no-branching which can be defined as:

$$P_{\mathrm{a}}(t) = \Gamma_{\mathrm{a}}(t) e^{\left(-\int_{t_0}^{t} dt' \Gamma_{\mathrm{a}}(t')\right)} \tag{2.10}$$

The factor $e^{\left(-\int_{t_0}^{t} dt' \Gamma_{\mathrm{a}}(t')\right)}$ is the so-called Sudakov form factor which expresses the probability for a parton a at an initial scale t_0 to evolve without any branching to a successive scale t. The quantity P_a(t) indicates the probability for the parton of evolving without any branching from t_0 to t, and of splitting at exactly the scale t. The function $\Gamma_{\mathrm{a}}(t')$ contains in its definition the parton evolution. In an event generator, the evolution starts at the hard scattering and proceeds backwards to lower scales. All the partons at the end of the evolution experience the hadronization process.

The matching between the matrix element and the PS can be performed in different ways (see Sect. 2.2.1).

In this thesis, the following event generators have been used for predictions to be compared to the measurements[8]:

- PYTHIA6 and PYTHIA8 [58, 59]: a LO $2 \to 2$ ME, matched with a DGLAP evolution at an approximate Next-to-Leading-Log level (NLL) for the simulation of the PS is generated; in this approximation, terms up to $P^0(z)$ are resummed to all orders of α_S of the evolution, with colour coherence and energy-momentum conservation constraints.[9] The PS is ordered in transverse momentum of the emitted partons: this means that partons with decreasing p_T are successively emitted. Initial-state radiation is generated with a backward evolution: this means that first, the hard scattering is calculated and then the incoming partons are evolved backwards down to a low scale. The hadronization is performed with the string model and the UE is simulated with specific sets of parameters which regulate colour reconnection and MPI contribution, determined by fits to measurements at colliders;
- HERWIG++ 2.5 [60]: like in PYTHIA, a LO $2 \to 2$ ME is generated; the PS is simulated by using DGLAP evolution, where the shower is angular-ordered: this means that the radiation is generated coherently inside the splitting cones of the partons. The hadronization follows the cluster model and the UE is tuned to data;
- MADGRAPH 5 [61, 62]: a LO $2 \to 2+n$ ME, where n is the number of additional partons included in the analytical calculation of the hard scattering is generated. It does not simulate any PS or UE contributions, which are provided by interfacing it with either PYTHIA or HERWIG++, generally through the MLM method [12];
- POWHEG [13, 63]: based on the POWHEG box [64], a NLO $2 \to 2$ ME, with an additional parton included in the matrix element, is generated. Again this generator does not include PS and UE which need to be borrowed by interfacing POWHEG

[8] A brief description of the main features used is given here for every generator. More information can be found in the quoted references.

[9] This is why it is not just LLA but approximate NNL.

Table 2.1 Summary of the event generators used in this thesis for comparison with the measurements: the matrix element, the parton evolution and the hadronization models used by each of them are also listed.

Monte Carlo event generator	Matrix element	Parton shower	Hadronization
PYTHIA	LO $2 \to 2$	DGLAP	String
HERWIG++	LO $2 \to 2$	DGLAP	Cluster
MADGRAPH	LO $2 \to 2$+n	-	-
POWHEG	NLO $2 \to 2 + 1$ hard jet	-	-
SHERPA	LO $2 \to 2$+n	DGLAP	Cluster

with PYTHIA or HERWIG++. The ME-PS matching is performed with the POWHEG method;

- SHERPA [65]: similar to MADGRAPH, a LO $2 \to 2+n$ ME is generated, but PS and UE simulation is also included. The PS follows the DGLAP evolution and it is matched to the ME with CKKM scheme. The type of hadronization used in the generator is the cluster model. Specific parameters are used for the UE in order to best describe available UE data.

A schematic summary of the matrix element used in the different generators in given in Table 2.1.

Note that only PYTHIA, HERWIG++ and SHERPA have their own UE generation, comprising PS, MPI and BBR. The MADGRAPH and POWHEG ME need to be interfaced to one of them for a full hadron-hadron collision simulation.

Since the work described in this thesis deals directly with MPI, in the following some current models of MPI are presented.

2.5.1 Models of Multiple Parton Interaction

In MC generators, the MPI have a key role for the description of the UE and Minimum Bias (MB) data, recorded in hadronic collisions. A big effort has been made to improve their modelling and further constrain the existing theories through comparison with the available measurements.[10] On one hand, this is important to better understand the internal proton structure, as well as the MPI mechanisms; on the other hand, the study of the contribution of MPI and DPS is fundamental to make predictions for any physics channel. In the following, the MPI models implemented in the most used MC generators are described.

[10] A wider treatment is given in Appendix D, where results of new UE tunes are described.

2.5.1.1 MPI in PYTHIA

The possibility that several parton pairs undergo simultaneous interactions is implemented in the PYTHIA event generator. The first necessary ingredient is the regularization of the partonic QCD cross section, $\hat{\sigma}$, which is divergent for $p_{\mathrm{T}} \to 0$. This is achieved by including the parameter p_{T_0} in the denominator, which removes the divergence, by modifying the dependence of $\hat{\sigma}$ on p_{T} in this way:

$$\frac{d\hat{\sigma}}{dp_{\mathrm{T}}^2} \propto \frac{\alpha_{\mathrm{S}}^2(p_{\mathrm{T}}^2)}{p_{\mathrm{T}}^4} \to \frac{\alpha_{\mathrm{S}}^2(p_{\mathrm{T}_0}^2 + p_{\mathrm{T}}^2)}{(p_{\mathrm{T}_0}^2 + p_{\mathrm{T}}^2)^2} \tag{2.11}$$

The parameter p_{T_0} is set to be energy-dependent and is controlled by two additional parameters, $p_{\mathrm{T}_0}^{\mathrm{ref}}$ and E_{pow}, in the generator. The energy dependence is expressed by the formula:

$$p_{\mathrm{T}_0} = p_{\mathrm{T}_0}^{\mathrm{ref}} \cdot \left(\frac{E}{E_{\mathrm{ref}}}\right)^{E_{\mathrm{pow}}} \tag{2.12}$$

The value of the energy reference, E_{ref}, is generally set in most of the tunes to 1800 GeV for historical reasons. This regularization is included in all MPI models implemented in PYTHIA. The basic idea of all models is that the average number of interactions per event is given by Eq. 2.5. The simultaneous interactions are assumed to be independent of each other and without any dependence on the relative position of the partons inside the hadrons. The PYTHIA event generator implements it by defining:

$$f(x_{\mathrm{T}}) = \frac{1}{\sigma_{\mathrm{nd}}(s)} \frac{d\sigma}{dx_{\mathrm{T}}} \tag{2.13}$$

that represents the probability to have a parton-parton interaction at a given $x_{\mathrm{T}} = 2p_{\mathrm{T}}/E_{\mathrm{cm}}$, given that the two hadrons undergo an inelastic collision. From this definition, a natural ordering in the hardness x_{T} of the scatterings is automatically set; the probability to have the hardest interaction at a scale x_{T_1} is obtained by:

$$P(x_{\mathrm{T}_1}) = f(x_{\mathrm{T}_1}) e^{\left\{-\int_{x_{T_1}}^1 f(x'_T) dx'_{\mathrm{T}}\right\}} \tag{2.14}$$

that includes the probability to have an interaction at x_{T_1} and not to have any interaction at scales larger than that value.[11] For the ith scattering, the probability is obtained by iteration:

$$P(x_{\mathrm{T}_i}) = \frac{f(x_{\mathrm{T}_i})}{(i-1)!} \left(\int_{x_{\mathrm{T}_i}}^1 f(x'_T) dx'_{\mathrm{T}}\right)^{\mathrm{i}-1} \cdot e^{\left\{-\int_{x_{T_1}}^1 f(x'_T) dx'_{\mathrm{T}}\right\}} \tag{2.15}$$

[11] This formalism uses the same concept of the Sudakov form factor in the parton evolution framework.

The chain of interactions terminates when $x_{\mathrm{T_i}}$ becomes smaller than $p_{\mathrm{T_{min}}}/E_{\mathrm{cm}}$.

In this mechanism, energy-momentum conservation becomes necessary and needs to be introduced. This is ensured by rescaling the parton distributions after every interaction by a factor:

$$x_{\mathrm{i}}' = \frac{1}{1 - \sum_{j=1}^{i=1} x_{\mathrm{j}}} \tag{2.16}$$

This takes into account the energy already used in previous interactions and it decreases the amount of phase space available for further interactions, until no energy is left. For the hard scattering, namely the first interaction of the chain, the ordinary parton distributions are used.

Each MPI is associated with its set of initial- (ISR) and final-state (FSR) radiation as well as the partons participating in the hard scattering. In order to combine these different components, the previous formalism is implemented in an interleaved evolution between MPI, ISR and hard scattering process, following the equation given below:

$$\frac{dP}{dp_{\mathrm{T}}} = \left(\frac{dP_{\mathrm{MPI}}}{dp_{\mathrm{T}}} + \sum \frac{dP_{\mathrm{ISR}}}{dp_{\mathrm{T}}}\right) \cdot e^{\left(-\int_{p_{\mathrm{T}}}^{p_{\mathrm{T_{i-1}}}} \left(\frac{dP_{\mathrm{MPI}}}{dp_{\mathrm{T}}'} + \sum \frac{dP_{\mathrm{ISR}}}{dp_{\mathrm{T}}'}\right) dp_{\mathrm{T}}'\right)} \tag{2.17}$$

where $p_{\mathrm{T_i}}$ is the transverse momentum of the ith interaction or parton branching (for a pictorial view, see Fig. 2.8 (left)). Note the similarity of this equation with Eq. 2.10; it differs from that, only because initial-state radiation is also included in the formalism.[12] The FSR is included separately to the outgoing partons. While for the hard scattering all the processes can be generated, the additional interactions are limited only to QCD events, both initiated by quarks or gluons.

To take into account the possible different centralities of the collision, a dependence on the varying impact parameter is included. A small value of b corresponds to a large overlap between the colliding hadrons and consequently to a large probability of MPI, while large values for b refer to a smaller probability for parton-parton interactions. A double gaussian function is used for the overlap distribution:

$$\rho(r) \propto \frac{1-\beta}{a_1^3} e^{\left\{-\frac{r^2}{a_1^2}\right\}} + \frac{\beta}{a_2^3} e^{\left\{-\frac{r^2}{a_2^2}\right\}} \tag{2.18}$$

This corresponds to a distribution with a small core region, of radius a_2 and containing a fraction β of the total hadronic matter, embedded in a larger hadron of radius a_1. The choice of a double Gaussian function is motivated by comparisons with data of MB and UE hadronic activity [58]. Colour reconnection has been also

[12] In particular, if the hard scattering occurs at a scale $p_{\mathrm{T_1}}$, either a secondary hard interaction or a hard emission from an initial parton take place at the scale $p_{\mathrm{T_2}} < p_{\mathrm{T_1}}$.

included: this implements the possibility for colour strings coming from different interactions to be connected and exchange colour information; this idea is motivated by the fact that MPI tend to create lots of colour strings that most probably overlap in physical space and would be naturally connected.

These general features are implemented in the PYTHIA6 MPI model and very similarly in the SHERPA one. In PYTHIA8, a systematic improvement has been carried out by adding more sophisticated mechanisms, to get a more realistic picture of the MPI dynamics:

- the colour reconnection is performed by giving each system a probability to reconnect with a harder system defined as:

$$P = \frac{p^2_{\mathrm{T_{Rec}}}}{(p^2_{\mathrm{T_{Rec}}} + p^2_{\mathrm{T}})} \text{ with } p^2_{\mathrm{T_{Rec}}} = R \cdot p_{\mathrm{T_0}} \tag{2.19}$$

  where R is a parameter and $p_{\mathrm{T_0}}$ is the same quantity defined in Eq. 2.12;
- the rescattering [66]: this concept allows events where an outgoing state from one scattering becomes the initial state of another scattering, as represented in Fig. 2.8 (right);
- a richer range of generated MPI processes (photon, J/ψ, Drell-Yan production..);
- a wider set of overlap matter distribution functions, ranging from gaussian and double gaussian to an exponential low-x dependent function;
- a new interleaved evolution which includes also FSR together with ISR and MPI [67], based on the equation:

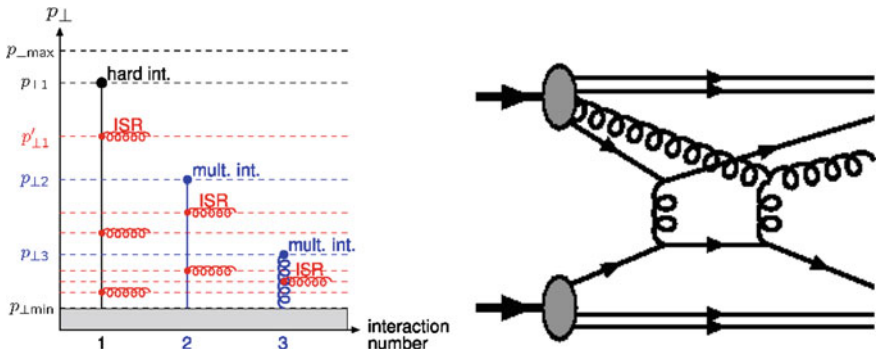


Fig. 2.8 (*Left*) Sketch of the interleaving evolution in PYTHIA6 [68]: the highest scale of the collision is set by the hard scattering. Then, hard emission and MPI are generated at successively decreasing scales. The formalism in PYTHIA8 is the same but it additionally considers also the FSR in the evolution. (*Right*) Example of a rescattering diagram [66]: a parton of one proton interacts with a parton of the other proton; from this interaction, two new partons are produced and one of which interacts again successively with another parton of the other proton

$$\frac{dP}{dp_{\mathrm{T}}} = \left(\frac{dP_{\mathrm{MPI}}}{dp_{\mathrm{T}}} + \sum \frac{dP_{\mathrm{ISR}}}{dp_{\mathrm{T}}} + \sum \frac{dP_{\mathrm{FSR}}}{dp_{\mathrm{T}}}\right) \cdot e^{\left(-\int_{p_{\mathrm{T}}}^{p_{\mathrm{T_{i-1}}}} \left(\frac{dP_{\mathrm{MPI}}}{dp'_{\mathrm{T}}} + \sum \frac{dP_{\mathrm{ISR}}}{dp'_{\mathrm{T}}} + \sum \frac{dP_{\mathrm{FSR}}}{dp'_{\mathrm{T}}}\right) dp'_{\mathrm{T}}\right)} \tag{2.20}$$

Furthermore, PYTHIA8 adds the possibility to generate manually two hard scatterings in the same event. Thanks to all these features, the MPI model in PYTHIA8, is believed to be the most complete. Hence, the PYTHIA8 event generator has been chosen for the preliminary sensitivity studies for the analyses presented in Chap. 4.

2.5.1.2 MPI in HERWIG++

Also HERWIG++ includes MPI [69] in order to simulate the UE. It is assumed that at fixed impact parameter b, individual scatterings are independent (only the momentum conservation is required, but no further constraints) and that the distribution of partons in the hadrons, factorizes with respect to the b and the x dependence. In this framework, the average number of hard interactions is given for hadronic collisions by:

$$n(b, s) = A(b, \mu^2)\sigma^{\mathrm{inc}}(s, p_{\mathrm{T}}^{\mathrm{min}}) \tag{2.21}$$

The function $A(b, \mu^2)$ describes the spatial overlap of the two colliding hadrons and the parameter μ is interpreted as the inverse radius of the proton; $p_{\mathrm{T_{min}}}$ sets the lower scale for allowed hard MPI. Below this threshold, soft non-perturbative MPI are also generated within the same model but they make use of a parametrization from the optical theorem in order to restore unitarity.

As in PYTHIA, this simple model is enriched by the introduction of colour reconnection that may cause non-trivial changes to the colour topology of the final state. In particular, parton jets emerging from different interactions are colour-connected if they are located closely in phase space. Inside the cluster hadronization model, the distance between two partons, namely the length of the colour connection, is related to the invariant mass of the cluster:

$$\lambda = \sum_{\mathrm{i}=1}^{\mathrm{N_i}} m_{\mathrm{i}}^2 \tag{2.22}$$

where the sum is performed over all the final clusters. The goal of CR is to reduce λ for every cluster. This mechanism is carried out in HERWIG++, by iterating over all possible cluster pairs and by finding the best association among the partons in the clusters, according to the minimum colour length. If the invariant mass of a new cluster is lower than the one of the previous cluster, a colour swap is applied with a certain probability. This model has been shown to improve the description of several observables, like the charged particle multiplicity [70].

References

1. Curci G et al (1980) Evolution of parton densities beyond leading order: the nonsinglet case. Nucl Phys B 175:27. doi:10.1016/0550-3213(80)90003-6
2. Lai H et al (2010a) New parton distributions for collider physics. Phys Rev D 82:074024. doi:10.1103/PhysRevD.82.074024
3. Pumplin J et al (2002) New generation of parton distributions with uncertainties from global QCD analysis. JHEP 0207:012. doi:10.1088/1126-6708/2002/07/012
4. Aaron FD et al (2010) Combined measurement and QCD analysis of the inclusive $e^{\pm}$p scattering cross sections at HERA. JHEP 1001:109. doi:10.1007/JHEP01(2010)109
5. Dittmar M et al (2009a) Parton distributions. hep-ph/0901.2504
6. Beringer J et al (2012a) Review of particle physics (RPP). Phys Rev D 86:010001. doi:10.1103/PhysRevD.86.010001
7. Skands P (2012) Introduction to QCD. hep-ph/1207.2389
8. Ruiz R (2011) Feynman diagrams images, produced with the FeynLib and JaxoDraw software. http://home.fnal.gov/~rruiz/FeynLib/
9. Andersen JR et al (2010c) The SM and NLO multileg working group: summary report, pp 21–189
10. Hoeche S et al (2006a) Matching parton showers and matrix elements. hep-ph/0602031
11. Lönnblad L (2002) Correcting the color dipole cascade model with fixed order matrix elements. JHEP 0205:046. doi:10.1088/1126-6708/2002/05/046
12. Alwall J et al (2008a) Comparative study of various algorithms for the merging of parton showers and matrix elements in hadronic collisions. Eur Phys J C 53:473–500. doi:10.1140/epjc/s10052-007-0490-5
13. Frixione S et al (2007) Matching NLO QCD computations with parton shower simulations: the POWHEG method. JHEP 07:070. doi:10.1088/1126-6708/2007/11/070
14. Nason P, Webber B (2012) Next-to-leading-order event generators. Ann Rev Nucl Part Sci 62:187–213. doi:10.1146/annurev-nucl-102711-094928
15. Krauss F (2007) QCD and Monte Carlo tools. In: Talk at the CERN-Fermilab hadron collider physics summer schools
16. Ackerstaff K et al (1999) Measurements of flavor dependent fragmentation functions in Z0 → q anti-q events. Eur Phys J C 7:369–381. doi:10.1007/s100529901067
17. Chatrchyan S et al (2012b) Measurement of the underlying event in the Drell-Yan process in proton-proton collisions at $\sqrt{s} = 7$ TeV. Eur Phys J C 72:2080. doi:10.1140/epjc/s10052-012-2080-4
18. Chatrchyan S et al (2013) Measurement of the inelastic proton-proton cross section at $\sqrt{s} = 7$ TeV. Phys Lett B 722:5–27. doi:10.1016/j.physletb.2013.03.024
19. Aad G et al (2011a) Measurement of the Inelastic Proton-Proton Cross-Section at $\sqrt{s} = 7$ TeV with the ATLAS Detector. Nature Commun 2:463. doi:10.1038/ncomms1472
20. Kovner A, Wiedemann UA (2003) Taming the BFKL intercept via gluon saturation. Nucl Phys A 715:871–874. doi:10.1016/S0375-9474(02)01529-4
21. CTEQ workshop (2013) From 8 to 14 TeV: What's needed and why? http://tigger.uic.edu/~varelas/cteq/workshop_2013/
22. Acosta D et al (2004) The underlying event in hard interactions at the Tevatron $\bar{p}p$ collider. Phys Rev D 70:072002. doi:10.1103/PhysRevD.70.072002
23. Field R et al (2001) Defining maximum and minimum transverse regions to study the underlying event in hard scattering processes. In: CDF Note CDF/ANAL/MIN_BIAS/CDFR/5626
24. Aaltonen T et al (2010d) Studying the underlying event in drell-yan and high transverse momentum jet production at the tevatron. Phys Rev D 82:034001. doi:10.1103/PhysRevD.82.034001
25. Chatrchyan S et al (2011b) Measurement of the underlying event activity at the LHC with $\sqrt{s} = 7$ TeV. JHEP 1109:109. doi:10.1007/JHEP09(2011)109
26. Aad G et al (2011c) Measurement of underlying event characteristics using charged particles in pp collisions at $\sqrt{s} = 900GeV$ and 7 TeV with the ATLAS detector. Phys Rev D 83:112001. doi:10.1103/PhysRevD.83.112001

27. CMS Collaboration (2013a) Study of the underlying event, b-quark fragmentation and hadronization properties in $t\bar{t}$ events. In: CMS-PAS-TOP-13-007
28. Delabat Y (2013) Monte Carlo study of the underlying event in b-quark pair production with the CMS detector at the LHC. In: DESY summer student 2013 report, Sept 2013
29. CMS Collaboration (2014) Measurement of azimuthal correlations between forward and central jets in proton proton collisions at $\sqrt{s} = 7$ TeV. In: CMS-PAS-FSQ-12-008
30. Chatrchyan S et al (2014a) Measurement of pseudorapidity distributions of charged particles in proton-proton collisions at $\sqrt{s} = 8$ TeV by the CMS and TOTEM experiments
31. Chatrchyan S et al (2011d) Measurement of energy flow at large pseudorapidities in pp and 7 TeV. JHEP 1111:148. doi:10.1007/JHEP11(2011)148,10.1007/JHEP02(2012)055
32. Paver N, Treleani D (1982) Multi—Quark scattering and large p_T jet production in hadronic collisions. Nuovo Cim A 70:215. doi:10.1007/BF02814035
33. Halzen F et al (1987) Evidence for multiple parton interactions from the observation of multi—muon events in Drell-Yan experiments. Phys Lett B 188:375–378. doi:10.1016/0370-2693(87)91400-6
34. Berger E et al (2010e) Characteristics and estimates of double parton scattering at the large hadron collider. Phys Rev D 81:014014. doi:10.1103/PhysRevD.81.014014
35. Humpert B, Odorico R (1985) Multiparton scattering and QCD radiation as sources of four jet events. Phys Lett B 154:211. doi:10.1016/0370-2693(85)90587-8
36. Ametller L et al (1986) Possible signature of multiple parton interactions in collider four jet events. Phys Lett B 169:289. doi:10.1016/0370-2693(86)90668-4
37. Godbole RM et al (1990) Double parton scattering contribution to W+jets. Z Phys C47:69. doi:10.1007/BF01551914
38. Hussein MY (2007) Double parton scattering in associate Higgs boson production with bottom quarks at hadron colliders. hep-ph/0710.0203
39. Kom CH et al (2011e) Pair production of J/psi as a probe of double parton scattering at LHCb. Phys Rev Lett 107:082002. doi:10.1103/PhysRevLett.107.082002
40. Calucci G et al (2013b) Double parton scatterings in high-energy proton-nucleus collisions and partonic correlations. hep-ph/1309.6201
41. Blok B et al (2013c) Hard four-jet production in pA collisions. Eur Phys J C 73(6):2433. doi:10.1140/epjc/s10052-013-2433-7
42. Bahr M et al (2013) Extracting sigma_effective from the CDF gamma+3jets measurement. JHEP 1303:129. doi:10.1007/JHEP03(2013)129
43. Seymour MH, Siodmok A (2013) Extracting sigma_effective from the LHCb double-charm measurement. hep-ph/1308.6749
44. Gaunt JR, Stirling WJ (2010) Double parton distributions incorporating perturbative QCD evolution and momentum and quark number sum rules. JHEP 1003:005. doi:10.1007/JHEP03(2010)005
45. Blok B et al (2012c) pQCD physics of multiparton interactions. Eur Phys J C 72:1963. doi:10.1140/epjc/s10052-012-1963-8
46. Transverse Strikman M, Structure Nucleon, Interactions Multiparton (2011) Acta Phys Polon B 42:2607–2630. doi:10.5506/APhysPolB.42.2607
47. Diehl M et al (2014) Correlations in double parton distributions: effects of evolution. JHEP 1405:118. doi:10.1007/JHEP05(2014)118
48. Manohar AV, Waalewijn WJ (2012) A QCD analysis of double parton scattering: color correlations, interference effects and evolution. Phys Rev D 85:114009. doi:10.1103/PhysRevD.85.114009
49. Diehl M (2014) Multiple hard scattering and parton correlations in the proton. hep-ph/1411.0847
50. Diehl M, Schäfer A (2011) Theoretical considerations on multiparton interactions in QCD. Phys Lett B 698:389–402. doi:10.1016/j.physletb.2011.03.024
51. Collaboration AFS (1987) Double parton scattering in pp collisions at $\sqrt{s}$ = 63 GeV. Z Phys C 34:163

52. D0 Collaboration (2010) Double parton interactions in photon+3 jet events in $p\bar{p}$ = 1.96 TeV. Phys Rev D 82:114030
53. Abe F et al (1997) Double parton scattering in $\bar{p}p$ collisions at $\sqrt{s}$ = 1.8 TeV. Phys Rev D 56:3811. doi:10.1103/PhysRevD.56.3811
54. Aad G et al (2013e) Measurement of hard double-parton interactions in $W(\rightarrow l\nu)$+ 2 jet events at $\sqrt{s}$=7 TeV with the ATLAS detector. New J Phys 15:033038. doi:10.1088/1367-2630/15/3/033038
55. Chatrchyan S et al (2014) Study of double parton scattering using W + 2-jet events in proton-proton collisions at $\sqrt{s}$ = 7 TeV. JHEP 1403:032. doi:10.1007/JHEP03(2014)032
56. Abazov VM et al (2014d) Double parton interactions in photon + 3 jet and photon + b/c jet + 2 jet events in ppbar collisions at $\sqrt{s}$=1.96 TeV. Phys Rev D 89:072006. doi:10.1103/PhysRevD.89.072006
57. CMS Collaboration (2013b) Measurement of the prompt double J/psi production cross section in pp collisions at $\sqrt{s}$ = 7 TeV. In: CMS-PAS-BPH-11-021
58. Sjöstrand T et al (2006b) PYTHIA 6.4 physics and manual. JHEP 0605:026. doi:10.1088/1126-6708/2006/05/026
59. Sjöstrand T et al (2008) A brief introduction to PYTHIA 8.1. Comput Phys Commun 178:852–867. doi:10.1016/j.cpc.2008.01.036
60. Gieseke S et al (2011f) Herwig++ 2.5 release note. hep-ph/1102.1672
61. Maltoni F, Stelzer T (2003) MadEvent: automatic event generation with MadGraph. JHEP 02:027. doi:10.1088/1126-6708/2003/02/027
62. Alwall J et al (2011) MadGraph 5: going beyond. JHEP 06:128. doi:10.1007/JHEP06(2011)128
63. Nason P (2004) A new method for combining NLO QCD with shower Monte Carlo algorithms. JHEP 04:040. doi:10.1088/1126-6708/2004/11/040
64. Oleari C (2010) The POWHEG-BOX. Nucl Phys Proc Suppl 205–206:36. doi:10.1016/j.nuclphysbps.2010.08.016
65. Gleisberg T et al (2009b) Event generation with SHERPA 1.1. JHEP 02:007. doi:10.1088/1126-6708/2009/02/007
66. Corke R, Sjöstrand T (2010) Multiparton interactions and rescattering. JHEP 01:035. doi:10.1007/JHEP01(2010)035
67. Corke R, Sjöstrand T (2011) Interleaved parton showers and tuning prospects. JHEP 03:032. doi:10.1007/JHEP03(2011)032
68. Sjöstrand T (2005) New $p_\perp$-ordered showers and Interleaved multiple interactions. In: Talk at the ATLAS week
69. Gieseke S et al (2013f) Multiple partonic interactions in Herwig++. Acta Phys Polon Supp 6:613–620. doi:10.5506/APhysPolBSupp.6.613
70. Gieseke S et al (2012d) Colour reconnections in Herwig++. Eur Phys J C 72:2225. doi:10.1140/epjc/s10052-012-2225-5

http://www.springer.com/978-3-319-22212-7

Study of Double Parton Scattering Using Four-Jet Scenarios
in Proton-Proton Collisions at sqrt s = 7 TeV with the CMS Experiment at the LHC
Gunnellini, P.
2016, XX, 279 p. 125 illus., 55 illus. in color., Hardcover
ISBN: 978-3-319-22212-7